論文 / 著書情報
Article / Book Information

Title	Preparation of Y2O3:Er,Yb nanoparticles by laser ablation in liquid
Authors	T. Nunokawa, Y. Onodera, M. Hara, Y. Kitamoto, O. Odawara, H. Wada
Citation	Applied Surface Science, Vol. 261, No. , pp. 118-122
Pub. date	2012, 11
DOI	10.1016/j.apsusc.2012.07.110
Creative Commons	The information is in the article.
Note	このファイルは著者（最終）版です。 This file is author (final) version.

License

Title:

Preparation of Y_2O_3:Er,Yb Nanoparticles by Laser Ablation in Liquid

Author names and affiliations:

Takashi Nunokawa, Yuji Onodera, Masahiko Hara, Yoshitaka Kitamoto, Osamu Odawara, Hiroyuki Wada

Interdisciplinary Graduate School of Science and Engineering, Tokyo Institute of Technology, 4259 Nagatsuta-cho, Midoriku, Yokohama 226-8502, Japan

Corresponding author:

Takashi Nunokawa

Phone/Fax: +81-45-924-5567

E-mail: nunokawa.t.aa@m.titech.ac.jp,

Postal address: #J2-41, 4259 Nagatsuta-cho, Midoriku, Yokohama 226-8502, Japan

Abstract

We prepared a Y_2O_3:Er,Yb nanoparticles by laser ablation in liquid. The laser used the second harmonic generation Nd:YAG (532 nm). A preparation process and measurement of upconversion properties were performed by varying the range of the energy density of the laser. Images from scanning electron microscopy (SEM) indicated that two types of nanoparticles existed in the product of laser ablation in liquid. We concluded the following: one type of nanoparticles was prepared from the nucleation of materials in a plume and the other was prepared by fragmentation. In the photoluminescence spectra, green ($^2H_{11/2}$, $^4S_{3/2} \rightarrow {}^4I_{15/2}$) and red ($^4F_{7/2} \rightarrow {}^4I_{15/2}$) fluorescence were observed using a 980 nm laser diode (LD) as the excitation source. We confirmed that the fluorescence intensity increased with increasing energy density of the laser. Thus, we concluded that the number of the nanoparticles increased as the energy density of the laser was increased.

Keywords

Nanoparticle, Upconversion, Y_2O_3, Laser ablation, Nanosecond laser

1. Introduction

In recent years, rare-earth doped fluorescent materials have attracted much attention because of their unique optical properties and potential applications in the field of bio-imaging, color displays, and optical communications [1-5]. Articles on the upconversion fluorescent properties of rare-earth doped Y_2O_3 have been reported. The upconversion fluorescent materials are substances that emit visible light by irradiating near infrared as an exciting light [6-8]. Activators, such as Er^{3+}, Tm^{3+}, Ho^{3+}, and Pr^{3+}, function as the upconversion fluorescent materials [9-13]. Light of various colors is emitted depending on the rare-earth ions. Because Yb^{3+} has energy bands at 980 nm ($^2F_{5/2} \rightarrow {}^2F_{7/2}$), it is often used as an effective sensitizer. In particular, Y_2O_3 as a host material has the same crystal structure as Er_2O_3 and Yb_2O_3 [14-16]. Y_2O_3 includes a comparatively high refractive index, low phonon energy, and high chemical and thermal stability.

Thus far, the chemical synthetic methods, such as solid state, hydrothermal, coprecipitation, and sol-gel methods, are well-known for preparing the upconversion nanoparticles [17-22]. In these methods, however, nanoparticles are easily aggregated by heating processes. It has been difficult to prepare the finely dispersed nanoparticles, and new synthetic methods are needed. Additionally, nanoparticles have been prepared in the gas-phase. Laser ablation, such as pulse laser deposition (PLD), has often been studied by researchers who fabricate nanoparticles on various targets [23-25].

We focused on laser ablation in liquid. This technology is for preparing the colloidal solution by irradiating the targets with a pulsed laser beam in liquid. Laser ablation in liquid has many advantages: the nanoparticles are formed easily; the nanoparticles are collected with high efficiency compared with preparation in the gas phase; and pure colloidal solutions can be prepared, compared with general chemical synthesis methods. Recently, many researchers have studied laser ablation in liquid, and various materials have been irradiated with this technology. Cotton et al. prepared a colloidal solution by irradiating the metal targets with a laser [26]. Mafune et al. prepared Au nanoparticles in a surfactant [27,28]. Hosokawa et al. irradiated organic materials with laser ablation [29]. Koshizaki et al. prepared a colloidal solution containing ceramics using this technology [30]. However, no research has yet been performed to prepare the upconversion colloidal solution by laser ablation in liquid.

In this study, a Y_2O_3:Er,Yb colloidal solution was prepared by laser ablation in liquid. We used nanosecond laser pulses in the preparation of the nanoparticles. We investigated the relations between the particle size of the upconversion nanoparticles and the energy density of laser ablation in liquid. Subsequently, we evaluated the performance of the process by viewing the samples with a scanning electron microscope (SEM) and a transmission electron microscope (TEM). Additionally, the optical properties of the upconversion nanoparticles were measured with fluorescence spectrophotometer.

2. Experimental methods

2.1 Preparation of the target

$Y(NO_3)_3 \cdot 6H_2O$ (99.99% Kanto Chemical Co., Inc.), $Er(NO_3)_3 \cdot 5H_2O$ (99.9% Mitsuwa's Pure Chemicals), $Yb(NO_3)_3 \cdot 5H_2O$ (99.9% Wako Pure Chemical Industries, Ltd.), and aqueous ammonia (28% Kanto Chemical Co., Inc.) were used as starting materials. We completely dissolved $Y(NO_3)_3 \cdot 6H_2O$ (11.1 mmol), $Er(NO_3)_3 \cdot 5H_2O$ (0.125 mmol) and $Yb(NO_3)_3 \cdot 5H_2O$ (1.25 mmol) with deionized water. Aqueous ammonia (11 mL) was added dropwise to this solution. The prepared solution was aged for 24 h. The precipitations were dried at 900 °C for 2 h. The dried powder was pressed into shapes and sintered at 1250 °C for 4 h. The targets were 9 mm in diameter and 3 mm in height.

An overview of the synthesis scheme is given by the following reaction steps:

$$RE(NO_3)_3 + 3NH_4OH \rightarrow RE(OH)_3 + 3NH_4NO_3 \quad (1)$$

$$2RE(OH)_3 \xrightarrow{900\ ^\circ C} RE_2O_3 + 3H_2O \quad (2)$$

where RE indicates Y, Er, Yb.

2.2 Preparation of the colloidal solution

The Y_2O_3:Er,Yb colloidal solution was prepared by laser ablation in liquid. The target was placed on the bottom of the cell that was filled with 2 ml of deionized water. The Nd:YAG laser (Spectron Laser Systems Ltd., SL8585G) served as a light source for pulsed

laser ablation and was operated with the second harmonic generation (wavelength: 532 nm) at a laser energy of 23.1 mJ/pulse and a repetition rate of 10 Hz. The average energy density of the laser was varied in the range of 0.20 – 1.61 J/cm^2. The pulse width was 13 ns when measured with a fast PIN photodiode and a digital oscilloscope. The target was irradiated with the laser for 30 min.

2.3 Characterizations

We characterized the composition of the synthesized target and the prepared nanoparticles with an X-ray diffractometer (XRD, PANalytical X'pert-PRO-MRD). The average particle size was measured by Dynamic Light Scattering (DLS, Sysmex Co. Zetasizer Nano). The laser source of the DLS was a He-Ne laser (633 nm). The configuration of the nanoparticles was observed by scanning electron microscopy (SEM, Hitachi High-Technologies Co. S-4800) and transmission electron microscopy (TEM, JEOL Ltd. JEM-1010BS). The colloidal solution of Y_2O_3:Er,Yb was placed onto the elastic carbon supporting film. A powder of the Y_2O_3:Er,Yb targets was placed on a microscope stage. The elemental analysis of the nanoparticles was performed by energy dispersive X-ray (TEM-EDX) spectroscopy. Under irradiation with a 980 nm laser diode (LD), upconversion properties were measured using a fluorescent spectrophotometer (Hitachi High-Technologies Co. F-7000).

3. Result and discussion

Figure 1 shows the XRD patterns of Y_2O_3:Er,Yb in the synthesized targets and the prepared nanoparticles. The vertical bars below the patterns represent the standard diffraction data (ICDD-PDF-4 No. 01-079-1716). The synthesized targets and the prepared nanoparticles had a space group Ia3 of the C-type Y_2O_3 structure. These nanoparticles were prepared at an average energy density of 4.2 J/cm^2. We found that the crystal phase of the nanoparticles prepared by laser ablation in liquid was the same as that of the targets. No additional peaks representing other phases were observed.

Figure 2 shows the particle size as a function of the average energy density in laser ablation in liquid. The particle size was measured with DLS. This particle size was calculated from the scattering intensity of the fluctuation, which is dependent on the Brownian motion of the particle. The size distribution of DLS is provided in the supporting information (SI1). We found that the particle size increased with the increasing energy density of the laser. Yoshimura et al. showed a similar tendency [31].

We observed the configuration of the nanoparticles with SEM. In SEM images, nanoparticles on the order of 10^1 to 10^2 nm were observed. Figure 3 shows the SEM images of the synthesis targets and the nanoparticles prepared by laser ablation in liquid. Figure 3(a) shows the SEM images of the targets. Many aggregated nanoparticles on the order of a 10^2 nm

were observed. Figures 3(b), (c), and (d) show the SEM images of the nanoparticles. The average energy density in figures 3(b), (c), and (d) is 0.59, 1.06 and 1.61 J/cm^2, respectively. In 0.20 and 0.35 J/cm^2, the nanoparticles measuring on the scale of 10^2 nm nanometers were not observed. In the range between 0.59 and 1.61 J/cm^2, the nanoparticles on the scale of 10^2 nm were observed. During the preparation of the nanoparticles, the threshold average energy density ranged between 0.35 and 0.59 J/cm^2. We found that the particle size increased with increasing energy density of the laser in a similar manner as DLS. The nanoparticles were aggregated to each other. The size of the primary particles was nearly unchanged by the energy density. We found that the size and configurations of the nanoparticles measuring on the order of 10^2 nanometers was nearly the same as the size and configuration of the targets.

SEM images showed nanoparticles measuring on the order of 10^1 nm surrounding the larger nanoparticles. Figures 4(a) and (b) show the SEM images for the average energy densities of 0.59 and 1.61 J/cm^2, respectively. At 0.59 J/cm^2, dot-like nanoparticles were observed. At 1.61 J/cm^2, worm-like nanoparticles were observed. These worm-like nanoparticles are called often nano-strings [32].

Figure 5 shows the TEM images for the average energy density of the 1.61 J/cm^2. In Figure 4(b), nano-strings with lattice fringes were observed. The images confirmed that the direction of the lattice fringes varied. Figure 6 shows the EDX spectrum of the nano-strings. We performed an elemental analysis using the characteristic X-rays. The peaks of Y (K_{ab}, K_{β},

L_α), Yb (L_α, M), Er ($LIII_{ab}$, L_α, M) and O (K_α) were identified. Additional peaks for Cu and C were attributed to the carbon-coated copper grid. Based on these findings, we concluded that the nano-strings comprised Y, Yb, Er and O.

When targets are irradiated with a laser, a plume is prepared on the surface of the target [33,34]. Firstly, it has been known that a plume of high pressure was created on the target surface. The particles on the order of 10^2 nm would be prepared at high pressure by fragmentation of the target. On the contrary, in the particles on the order of 10^1 nm, nucleation would occur and they would be grown in the plume which consisted of materials such as atoms, electrons, ions and clusters. At low energy densities, the fine dot-like nanoparticles would be prepared. The number of dot-like nanoparticles increased with increased laser density. Subsequently, the dot-like nanoparticles were aggregated to each other. When a laser was irradiated again, the aggregated dot-like nanoparticles melted from the heat of laser. Finally, the nano-strings formed by these phenomena. S. Inasawa et al. also reported that nano-strings were prepared by laser irradiation [32].

Figure 7 shows the upconversion spectra of the nanoparticles prepared by varying the average energy density in laser ablation in liquid. The observation of green ($^2H_{11/2}$, $^4S_{3/2} \rightarrow {}^4I_{15/2}$) and red ($^4F_{9/2} \rightarrow {}^4I_{15/2}$) fluorescence of Er^{3+} was confirmed. Figure 8 shows the energy level diagrams of Er^{3+} and Yb^{3+}. In upconversion emission mechanisms, excited-state absorption (ESA) and energy-transfer excitation (ETU) have been reported [1-3]. A red

emission has been reported as follows: a 980 nm LD excites Er^{3+} from the ground state $^4I_{15/2}$ to the excited state $^4I_{11/2}$. Subsequently, a nonradioactive relaxation occurs from the $^4I_{11/2}$ level to the $^4I_{13/2}$ level. In the ESA, the photon energy of a 980 nm LD excites from the $^4I_{13/2}$ level to the $^4F_{9/2}$ level. In the ETU, the photon energy transfers from Yb^{3+} ($^2F_{5/2} \rightarrow {}^2F_{7/2}$) to the Er^{3+} ($^4I_{13/2} \rightarrow {}^4F_{9/2}$). Finally, the red emission is observed from the $^4F_{9/2} \rightarrow {}^4I_{15/2}$ transition in the Er^{3+}. Conversely, a green emission has been reported as follows: a 980 nm LD excites from the ground state $^4I_{15/2}$ to the excited state $^4I_{11/2}$. In the ESA, the photon energy of a 980 nm, LD excites from the $^4I_{11/2}$ level to the $^4F_{9/2}$ in the Er^{3+} level. In the ETU, the photon energy transfers from Yb^{3+} ($^2F_{5/2} \rightarrow {}^2F_{7/2}$) to the Er^{3+} ($^4I_{11/2} \rightarrow {}^4F_{7/2}$). Subsequently, a nonradioactive relaxation occurs from the $^4F_{7/2}$ level to the $^2H_{11/2}$ level or the $^4S_{3/2}$ level. Finally, the green emission is observed in the $^2H_{11/2}$, $^4S_{3/2} \rightarrow {}^4I_{15/2}$ transition.

Figure 9 shows the fluorescence intensity as a function of the average energy density of laser. We confirmed that the fluorescence intensity increased with increasing energy density of laser. The size of the primary particle only slightly changed as a result of altering the energy density as shown in Figure 3. One reason for the increase in the fluorescence intensity could be a reduction in the surface defects by the aggregated particles due to the passivation of the surface defects of nanoparticles [35,36]. However, the fluorescence intensity would be increased primarily because the number of the nanoparticles increased with the increasing energy density [37].

4. Conclusions

We successfully prepared Y_2O_3:Er,Yb nanoparticles by laser ablation in liquid. We observed the nanoparticles on the order of 10^1 to 10^2 nm in SEM images. We believe that the particles on the order of 10^2 nm were prepared by fragmentation. Conversely, the 10^1 nm scaled nanoparticles were prepared by a plume. Photoluminescent measurements indicated that the red ($^4F_{7/2} \rightarrow {}^4I_{15/2}$) and green ($^2H_{11/2}$, $^4S_{3/2} \rightarrow {}^4I_{15/2}$) fluorescence were emitted. We confirmed that the fluorescence intensity increased with the increasing energy density of the laser. We concluded that the number of the nanoparticles increased with the increasing energy density by laser ablation in liquid.

Acknowledgements

This work was carried out in Materials and Structure Laboratory (Tokyo Institute of Technology) as collaborative research. We would like to appreciate Prof. Kazutaka Nakamura for laser ablation. We would like to appreciate Mr. Yuichi Suzuki and Mr. Hiroshi Iida for XRD measurement and Mr. Katsuaki Hori for TEM measurement (Center for Advanced Materials Analysis, Tokyo Tech.).

References

[1] J. Zhou, Z. Liu, F. Li, Chem. Soc. Rev. 41 (2012) 1323-1351.

[2] T. Zako, H. Hyodo, K. Tsuji, K. Tokuzen, H. Kishimoto,; K. Ito, M. Maeda, K. Soga, J. Nanomater. 491471 (2010) pages 7.

[3] S. F. Lim, R. Riehn, W. S. Ryu. N. Khanarian, C. Tung, D. Tank, R, H, Austin, Nano. Letter. 6 (2006) 169-174.

[4] E. Downing, L. Hesselink, J. Raslton, R. Macfarlane, Science. 273 (1996) 1185-1189.

[5] M. B. Korzenski, P. Lecoeur, B. Merey, P. Camy, L. J. Doualan, Appl Phys Lett. 78 (2001) 1210-1212.

[6] F. Auzel., Chem. Rev. 104 (2004) 139-173.

[7] F. Auzel, F.C.R. Acad. Sci. (Paris) 262 (1966) 1016.

[8] F. Auzel, F.C.R. Acad. Sci. (Paris) 263B (1966) 819.

[9] J. A. Capobianco, F. Vetrone, J. C. Boyer, A. Speghini, M. Bettinelli, J. Phys. Chem. B. 106 (2002) 1181-1187.

[10] S. Chandra, F. L. Deepak, J. B. Gruber, D. K. Sardar, J. Phys. Chem. C. 114 (2010) 874-880.

[11] Q. Lü, F. GuoYun, L. Sun, A. Li, L. C. Zhao, J. Appl. Phys. 103 (2008) 123533.

[12] M. N. Sangeetha, F. Veggel. J. Phys. Chem. C. 113 (2009) 14702-14707.

[13] C. B. Zheng, Y. Q. Xia, F. Qin, Y. Yu, J. P. Miao, Z. G. Zhang, W. W. Cao, Chem. Phys. Lett. 496 (2010) 316-320.

[14] A. Ambrosini, A. Duarte, K. R. Poeppelmeier, M. Lane, C. R. Kannewurf, T. O. Mason, J. Solid. State. Chem. 153 (2000) 41-47.

[15] Z. Heiba, H. Okuyucu, Y. S. Hascicek, J. Appl. Crystallogr. 35 (2002) 577-580.

[16] C. Meyer, J. P. Sanchez, J. Thomasson, J. P. Itie, Phys. Rev. B; Condens. Matter. 51 (1995) 12187-12192.

[17] B. L. Cushing, V. L. Kolesnichenko, C. J. O'Connor, Chem. Rev. 104 (2004) 3893-3946.

[18] X. Hou, S. Zhou, T. Jia, H. Lin, H. Teng, J. Alloys. Compd. 509 (2011) 2793-2796.

[19] G. A. Kumar, M. Pokhrel, A. Martinez, R. C. Dennis, I. L. Villegas, D. K. Sardar. J. Alloys. Compd. 513 (2012) 559-565.

[20] X. Pei, Y. Hou, S. Zhao, Z. Xu. F.Teng, Mater. Chem. Phys. 90 (2005) 270-274.

[21] H. Du, W. Zhang, J. Sun, J. Alloys. Compd. 509 (2011) 3413-3418.

[22] V. B. Taxak, S. P. Khatkar, S. D. Han, R. Kumara, M. Kumara, J. Alloys. Compd. 469

(2009) 224-228.

[23] R. A.Ganeev, L. B. Elouga Bom, T. Ozaki, Appl. Phys. B. 96 (2009) 491-498.

[24] A. Huignard, A. Aron, P. Aschehoug, B. Viana, J. Thery, A. Laurent, J. Perriere, J. Mater. Chem. 10 (2000) 549-554.

[25] T. Takiya, I. Umezu, M. Yaga, M. Han, Journal of Physics: Conference Series, 59 (2007) 445-448.

[26] J. Neddersen, G. Chumanov, T. M. Cotton, Appl. Spectrosc. 47 (1993) 1959-1964.

[27] F. Mafune, J. Kohno, Y. Takeda, T. Kondow, H. Sawabe, J. Phys. Chem. B. 104 (2000) 9111-9117.

[28] F. Mafune, J. Kohno, Y. Takeda, T. Kondow, H. Sawabe, *J. Phys. Chem. B.* **2001**, 105, 5114-5120.

[29] Y. Hosokawa, M. Yashiro, T. Asahi, H. Fukumura, H. Masuhara, Appl. Surf. Sci. 154 (2000) 192-195.

[30] C. Liang, Y. Shimizu, T. Sasaki, N. Koshizaki, J. Mater. Res. 19 (2004) 1551-1557

[31] F. Y oshimura, K. Nakamura, F. Wakai, M. Hara, M. Yoshimoto, O. Odawara, H. Wada,

Appl. Surf. Sci. 257 (2011) 2170-2175.

[32] S. Inasawa, M. Sugiyama, Y. Yamaguchi, J. Phys. Chem. B. 109 (2005) 9404-9410.

[33] T. E. Itina, J. Phys. Chem. C. 115 (2011) 5044-5048.

[34] K. Sasaki, N. Takada, Pure Appl. Chem. 82 (2010) 1317-1327.

[35] Y. Wang, L. Tu, J, Zhao, Y. Sun, X. Kong, H. Zhang, J. Phys. Chem. C. 113 (2009) 7164-7169.

[36] F. Wang, J. Wang, X. Liu, Angew. Chem. Int. Ed. 49 (2010) 7456-7469.

[37] C. L. Sajti, R. Sattari, B. N. Chichkov, S. Barcikowski, J. Phys. Chem. C. 114 (2010) 2421-2427.

Figure captions

Figure 1. XRD pattern of targets (a), nanoparticles (b) and ICDD-PDF-4 No. 01-079-1716 of Y_2O_3.

Figure 2. Particle size as a function of the energy density for laser ablation in liquid.

Figure 3. SEM images of the targets and the nanoparticles. Targets (a), 0.59 J/cm^2 (b), 1.06 J/cm^2 (c), and 1.61(d) J/cm^2.

Figure 4. SEM images at an average energy density of 0.59 J/cm^2 (a) and 1.61 J/cm^2 (b).

Figure 5. TEM images of a nano-string.

Figure 6. EDX spectrum of the nano-string in Figure 5.

Figure 7. Upconversion spectra of nanoparticles. Energy density for laser ablation in liquid: solid line 1.61 J/cm^2, dot line 1.06 J/cm^2, broken line 0.59 J/cm^2, chain line 0.35 J/cm^2.

Figure 8. Energy level diagrams of Er^{3+} and Yb^{3+}.

Figure 9. Fluorescence intensity as a function of the energy density of the laser.

Supplementary data

We indicate figures of size distribution histograms of the upconversion nanoparticles by DLS measurement and SEM image in the average energy density of the 0.30 J/cm^2.

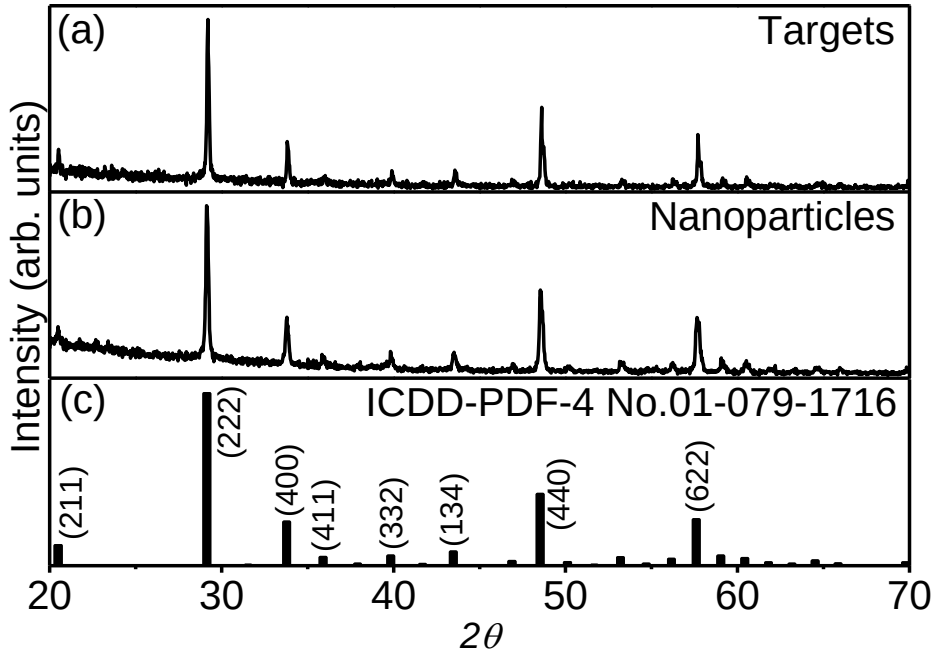

Figure 1. XRD pattern of targets (a), nanoparticles (b) and ICDD-PDF-4 No. 01-079-1716 of Y_2O_3.

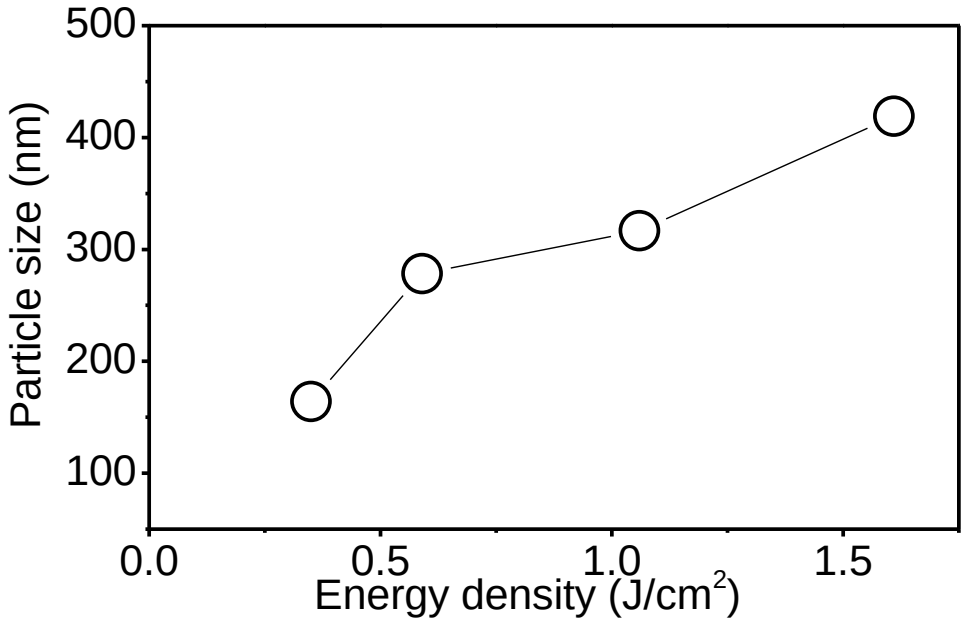

Figure 2. Particle size as a function of the energy density for laser ablation in liquid.

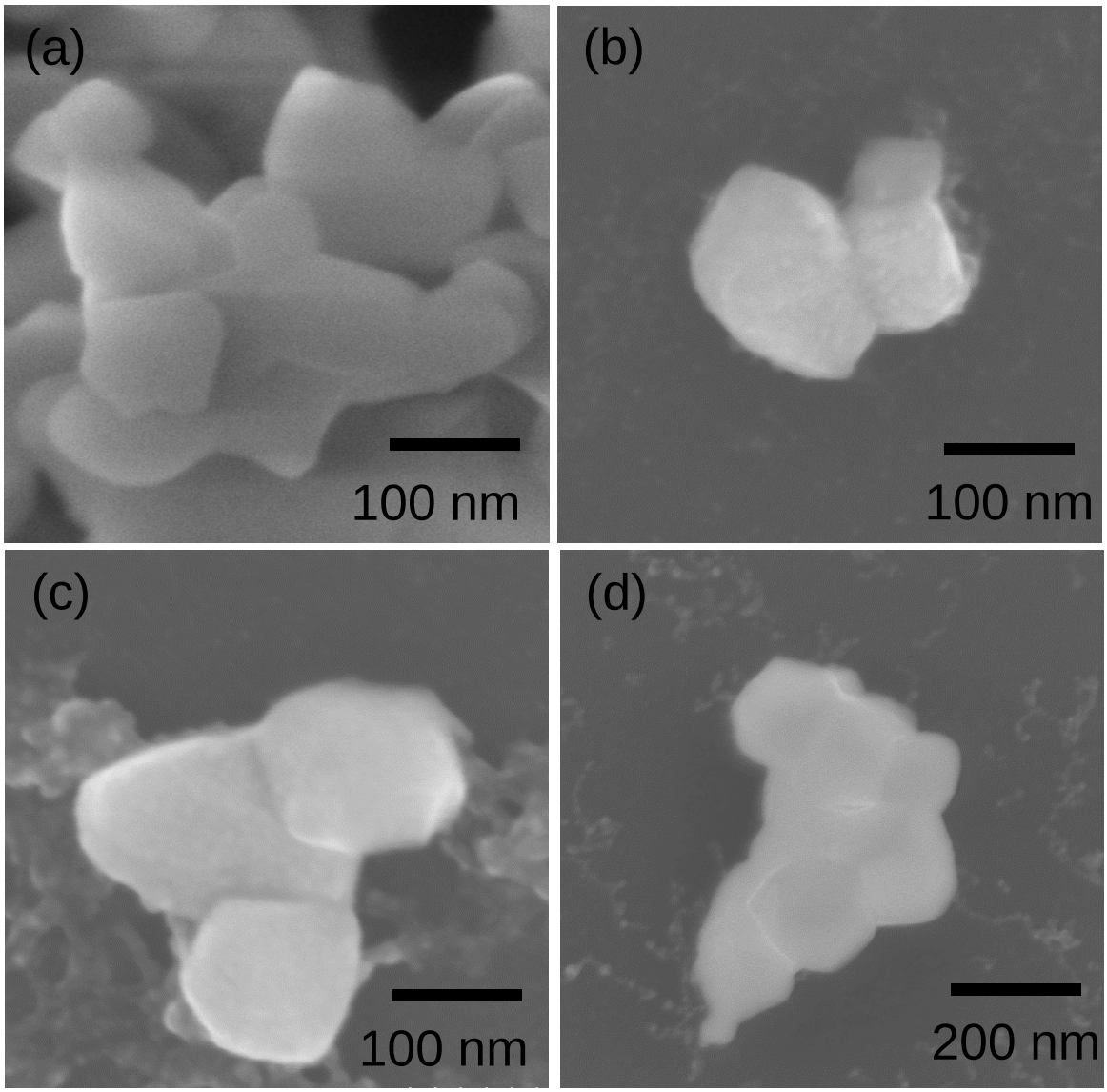

Figure 3. SEM images of the targets and the nanoparticles. Targets (a), 0.59 J/cm^2 (b), 1.06 J/cm^2 (c), and 1.61(d) J/cm^2.

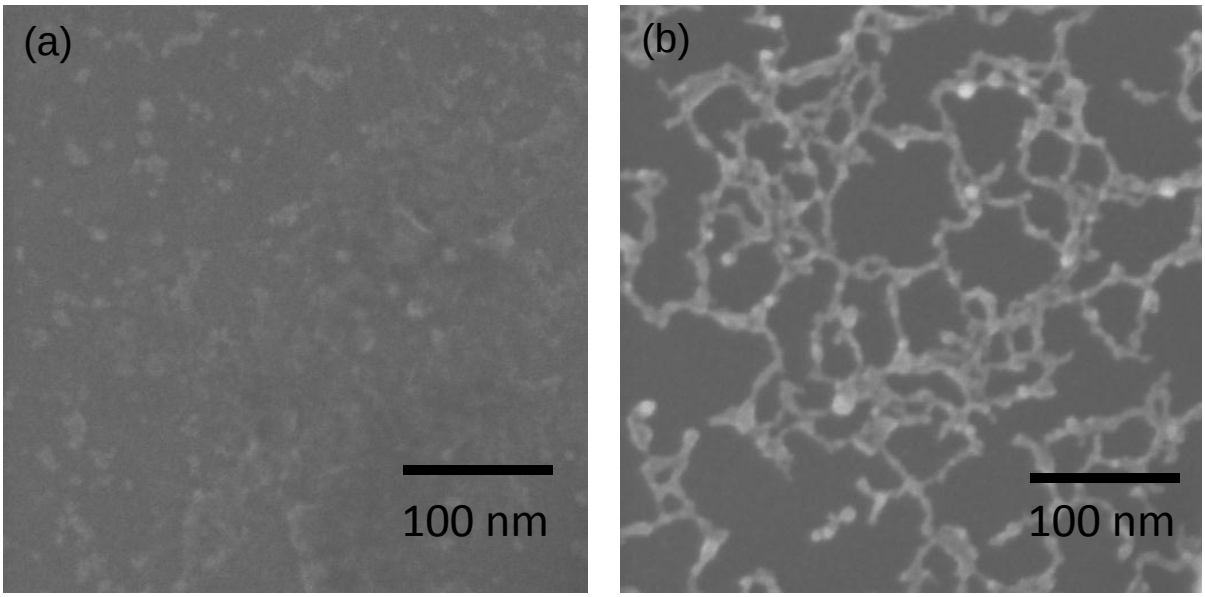

Figure 4. SEM images at an average energy density of 0.59 J/cm^2 (a) and 1.61 J/cm^2 (b).

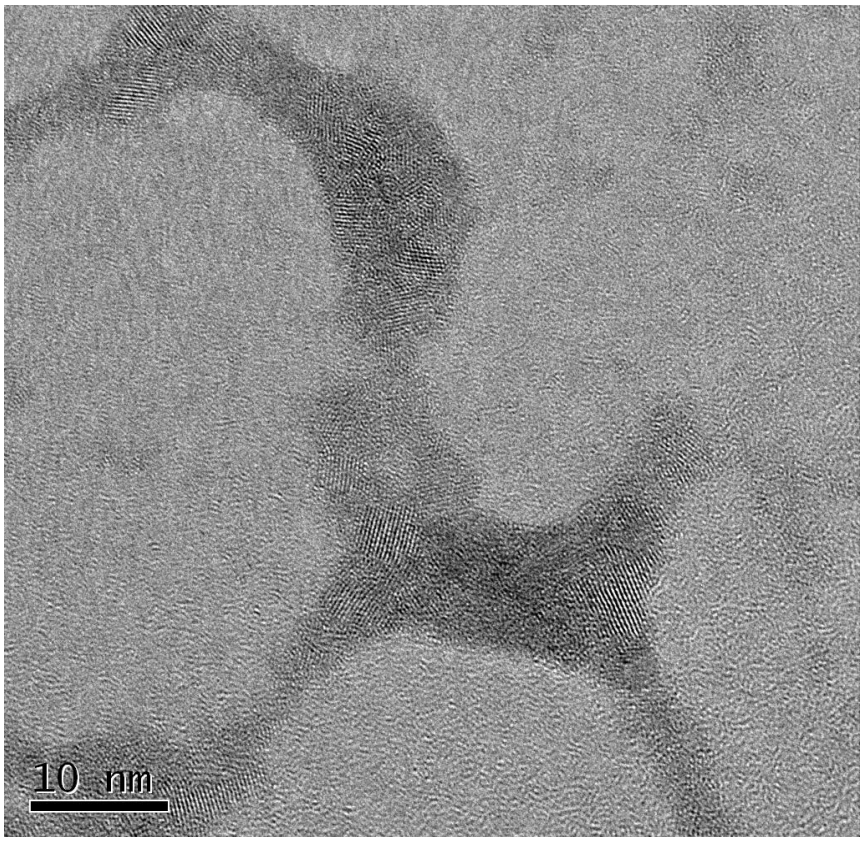

Figure 5. TEM images of a nano-string.

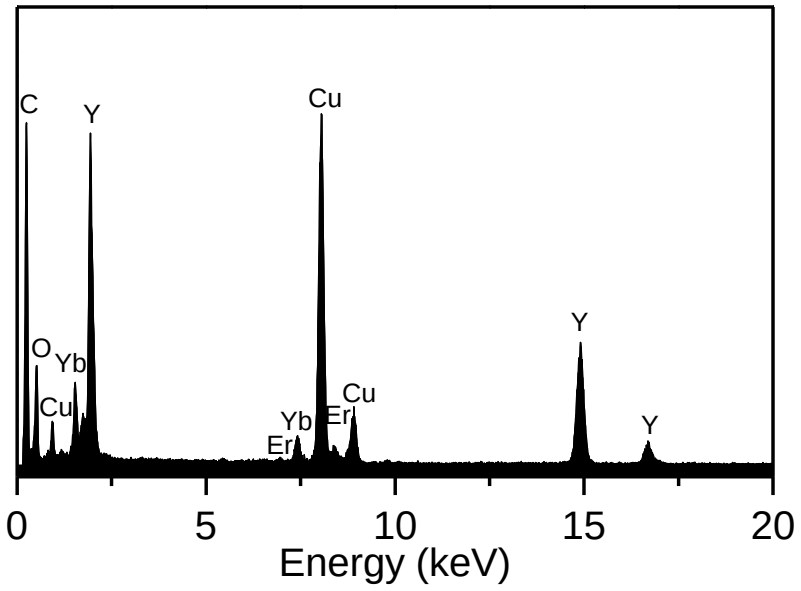

Figure 6. EDX spectrum of the nano-string in Figure 5.

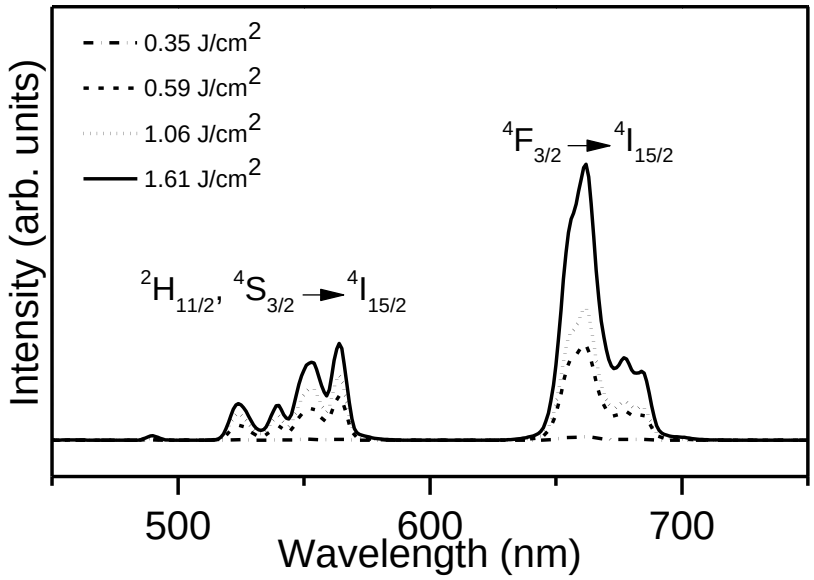

Figure 7. Upconversion spectra of nanoparticles. Energy density for laser ablation in liquid: solid line 1.61 J/cm^2, dot line 1.06 J/cm^2, broken line 0.59 J/cm^2, chain line 0.35 J/cm^2.

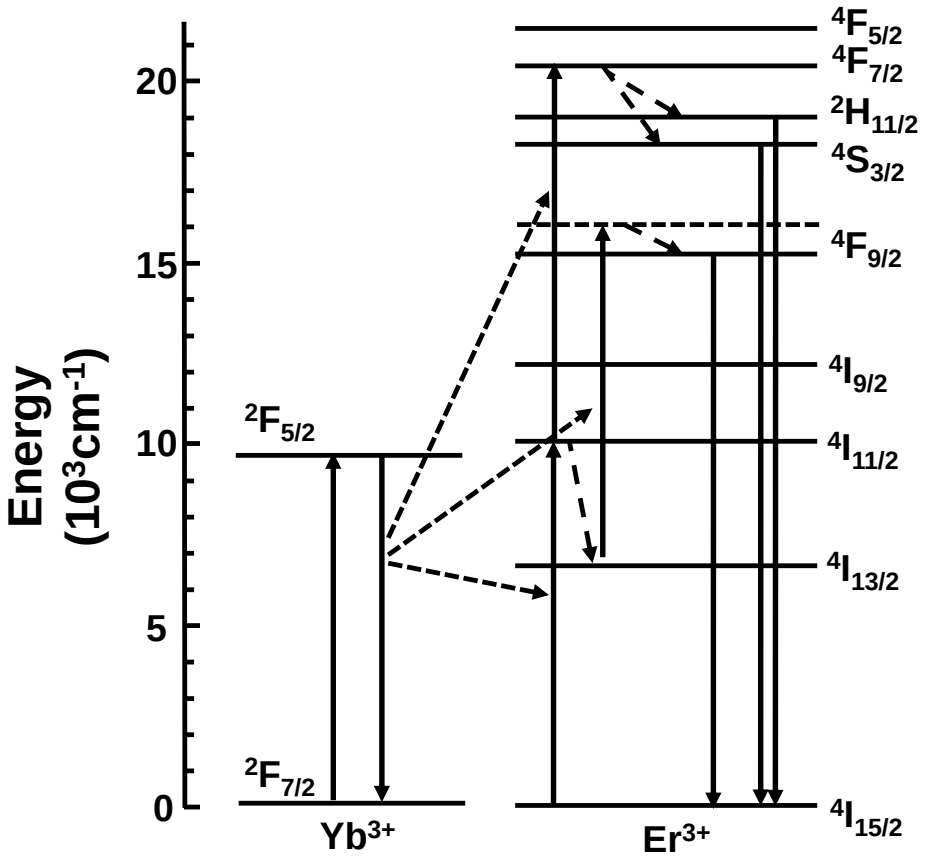

Figure 8. Energy level diagrams of Er^{3+} and Yb^{3+}.

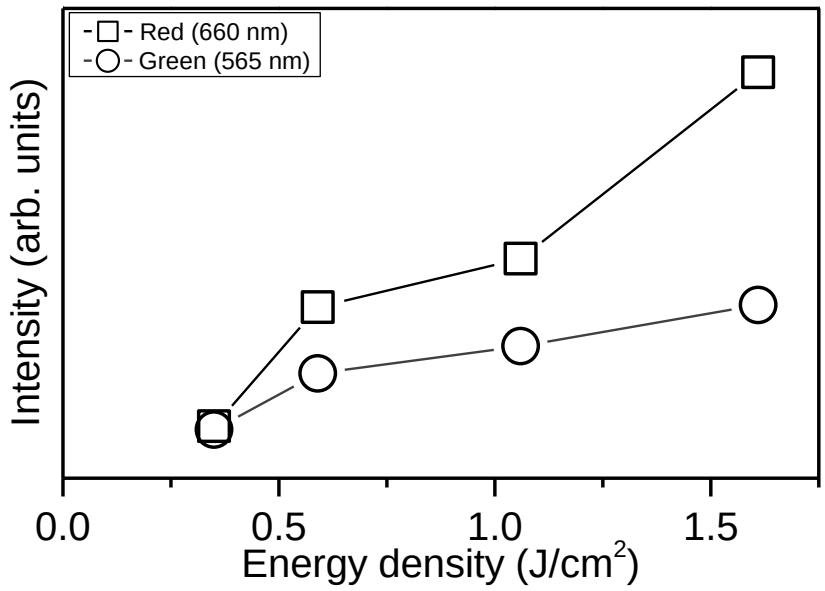

Figure 9. Fluorescence intensity as a function of the energy density of the laser.